Hindawi
Advances in High Energy Physics
Volume 2018, Article ID 5427158, 8 pages
https://doi.org/10.1155/2018/5427158

Research Article

Particle Motion around Charged Black Holes in Generalized Dilaton-Axion Gravity

Susmita Sarkar,[1] Farook Rahaman,[1] Irina Radinschi,[2] Theophanes Grammenos,[3] and Joydeep Chakraborty[4]

[1]*Department of Mathematics, Jadavpur University, Kolkata 700 032, West Bengal, India*
[2]*Department of Physics, Gheorghe Asachi Technical University, 700050 Iasi, Romania*
[3]*Department of Civil Engineering, University of Thessaly, 383 34 Volos, Greece*
[4]*Department of Mathematics, Nagar College, P.O. Nagar, Dist. Mursidabad, West Bengal, India*

Correspondence should be addressed to Farook Rahaman; rahaman@associates.iucaa.in

Received 14 May 2018; Accepted 8 August 2018; Published 16 September 2018

Academic Editor: Edward Sarkisyan-Grinbaum

The behaviour of massive and massless test particles around asymptotically flat and spherically symmetric, charged black holes in the context of generalized dilaton-axion gravity in four dimensions is studied. All the possible motions are investigated by calculating and plotting the corresponding effective potential for the massless and massive particles as well. Further, the motion of massive (charged or uncharged) test particles in the gravitational field of charged black holes in generalized dilaton-axion gravity for the cases of static and nonstatic equilibrium is investigated by applying the Hamilton-Jacobi approach.

1. Introduction

Recently, scientists have focused their attention on the black hole solutions in various alternative theories of gravity, particularly theories of gravitation with background scalar and pseudoscalar fields. In the low energy effective action, usually string theory based-models are comprised of two massless scalar fields, the dilaton, and the axion (see, e.g., [1]). Sur, Das, and SenGupta [2] employed the dilaton and axion fields coupled to the electromagnetic field in a more generalized coupling with Einstein and Maxwell theory in four dimensions in the low energy action. Exploiting this new idea, they have found asymptotically flat and nonflat dilaton-axion black hole solutions. The vacuum expectation values of the various moduli of compactification are responsible for these couplings. These black hole solutions have been studied extensively in the literature; e.g., their thermodynamics has been investigated [3], thin-shell wormholes have been constructed from charged black holes in generalized dilaton-axion gravity [4], the energy of charged black holes in generalized dilaton-axion gravity has been calculated [5], the statistical entropy of a charged dilaton-axion black hole has been examined [6], and the superradiant instability of a dilaton-axion black hole under scalar perturbation has been investigated [7]. Among various properties of such black hole solutions, a subject of great interest is the study of the behaviour of a test particle in the gravitational field of such black holes.

In this paper, we study the behaviour of the time-like and null geodesics in the gravitational field of a charged black hole in generalized dilaton-axion gravity. The solution under study describes an asymptotically flat black hole and the motions of both massless and massive particles are analyzed. The effective potentials are calculated and plotted for various parameters in the cases of circular and radial geodesics. The motion of a charged test particle in the gravitational field of a charged black hole in generalized dilaton-axion gravity is also investigated using the Hamilton-Jacobi approach.

The present paper has the following structure: in Section 2 the charged black hole metric in generalized dilaton-axion gravity is presented. Section 3 focuses on the geodesic equation in the cases of massless particle motion ($L = 0$) and massive particle motion ($L = -1$). In Section 4 the effective potential is studied in both cases of the massless and the massive particle. Section 5 is devoted to the study of the motion of a test particle in static equilibrium as well as in

nonstatic equilibrium. For the latter case, a chargeless ($e = 0$) and a charged test particle are considered. Finally, in Section 6, the results obtained in this paper are discussed.

2. Charged Black Hole Metric in Generalized Dilation-Axion Gravity

Recently, Sur, Das, and SenGupta [2] have discovered a new black hole solution for the Einstein-Maxwell scalar field system inspired by low energy string theory. In fact, they have considered a generalized action in which two scalar fields are minimally coupled to the Einstein-Hilbert-Maxwell field in four dimensions (in the Einstein frame, see, e.g., [8, 9]) having the form

$$I = \frac{1}{2\kappa}\int d^4x\sqrt{-g}\left[R - \frac{1}{2}\partial_\mu\varphi\partial^\mu\varphi - \frac{\omega(\varphi)}{2}\partial_\mu\zeta\partial^\mu\zeta - \alpha(\varphi,\zeta)F_{\mu\nu}F^{\mu\nu} - \beta(\varphi,\zeta)F_{\mu\nu}*F^{\mu\nu}\right], \tag{1}$$

where $\kappa = 8\pi G$, R is the curvature scalar, $F_{\mu\nu}$ describes the Maxwell field strength and φ, ζ are two massless scalar/pseudoscalar fields depending only on the radial coordinate r which are coupled to the Maxwell field through the functions α and β. Here, ζ acquires a nonminimal kinetic term of the form $\omega(\varphi)$ due to its interaction with φ (φ, ζ can be identified with the scalar dilaton field and the pseudoscalar axion field, respectively), while $*F^{\mu\nu} = (1/2)\varepsilon^{\mu\nu\kappa\lambda}F_{\kappa\lambda}$ is the Hodge-dual Maxwell field strength.

Indeed, with the action described by (1), a much wider class of black hole solutions has been found, whereby two types of metrics, asymptotically flat and asymptotically non-flat, for the black hole solutions have been obtained.

For our study we use the asymptotically flat solution to analyze the behaviour of massive and massless test particles around a spherically symmetric, charged black hole in generalized dilaton-axion gravity. The asymptotically flat metric considered is given by

$$ds^2 = -f(r)\,dt^2 + \frac{dr^2}{f(r)} + h(r)\,d\Omega^2, \tag{2}$$

with

$$f(r) = \frac{(r-r_-)(r-r_+)}{(r-r_0)^{(2-2n)}(r+r_0)^{2n}} \tag{3}$$

and

$$h(r) = \frac{(r+r_0)^{2n}}{(r-r_0)^{(2n-2)}}. \tag{4}$$

In (3) and (4), according to [2], in order to have nontrivial φ and ζ fields, the exponent n is a dimensionless constant strictly greater than 0 and strictly less than 1. The other various parameters are given as follows:

$$r_\pm = m_0 \pm \sqrt{m_0^2 + r_0^2 - \frac{1}{8}\left(\frac{K_1}{n} + \frac{K_2}{1-n}\right)}, \tag{5}$$

$$r_0 = \frac{1}{16m_0}\left(\frac{K_1}{n} - \frac{K_2}{1-n}\right), \tag{6}$$

$$m_0 = m - (2n-1)\,r_0, \tag{7}$$

$$K_1 = 4n\left[4r_0^2 + 2r_0(r_+ + r_-) + r_+r_-\right], \tag{8}$$

$$K_2 = 4(1-n)\,r_+r_-, \tag{9}$$

and

$$m = \frac{1}{16r_0}\left(\frac{K_1}{n} - \frac{K_2}{1-n}\right) + (2n-1)\,r_0, \tag{10}$$

where m is the mass of the black hole and $0 < n < 1$. The parameters r_+ and r_- determine the inner and outer event horizons, respectively. Also, for $r = r_0$, there is a curvature singularity and the parameters obey the condition $r_0 < r_- < r_+$.

3. Geodesic Equation

The geodesic equation for the metric (2) describing the motion in the plane $\theta = \pi/2$ is as follows [10]:

$$\left(\frac{dr}{d\tau}\right)^2 = Lf(r) + E^2 - \frac{J^2 f(r)}{h(r)}, \tag{11}$$

$$\frac{d\phi}{d\tau} = \frac{J}{h(r)}, \tag{12}$$

$$\frac{dt}{d\tau} = \frac{E}{f(r)}, \tag{13}$$

where L is known as the Lagrangian having the values 0 for a massless particle and -1 for a massive particle and E, J are constants identified as the energy per unit mass and the angular momentum, respectively.

Now we proceed to discuss the motion of the massless and the massive particle for the radial geodesic.

The radial geodesic equation ($J = 0$) is

$$\left(\frac{dr}{d\tau}\right)^2 = E^2 + Lf(r). \tag{14}$$

Using (13), (14) becomes

$$\left(\frac{dr}{dt}\right)^2 = (f(r))^2\left(1 + f(r)\frac{L}{E^2}\right). \tag{15}$$

Then, by inserting $f(r)$ from (3), (15) reads

$$\left(\frac{dr}{dt}\right)^2 = \left(\frac{(r-r_-)(r-r_+)}{(r-r_0)^{(2-2n)}(r+r_0)^{2n}}\right)^2 \cdot\left(1 + \frac{(r-r_-)(r-r_+)}{(r-r_0)^{(2-2n)}(r+r_0)^{2n}}\frac{L}{E^2}\right). \tag{16}$$

3.1. Massless Particle Motion ($L = 0$). For the motion of a massless particle the Lagrangian L vanishes. In this case the equation for the radial geodesic (16) becomes

$$\left(\frac{dr}{dt}\right)^2 = \left(\frac{(r-r_-)(r-r_+)}{(r-r_0)^{(2-2n)}(r+r_0)^{2n}}\right)^2. \tag{17}$$

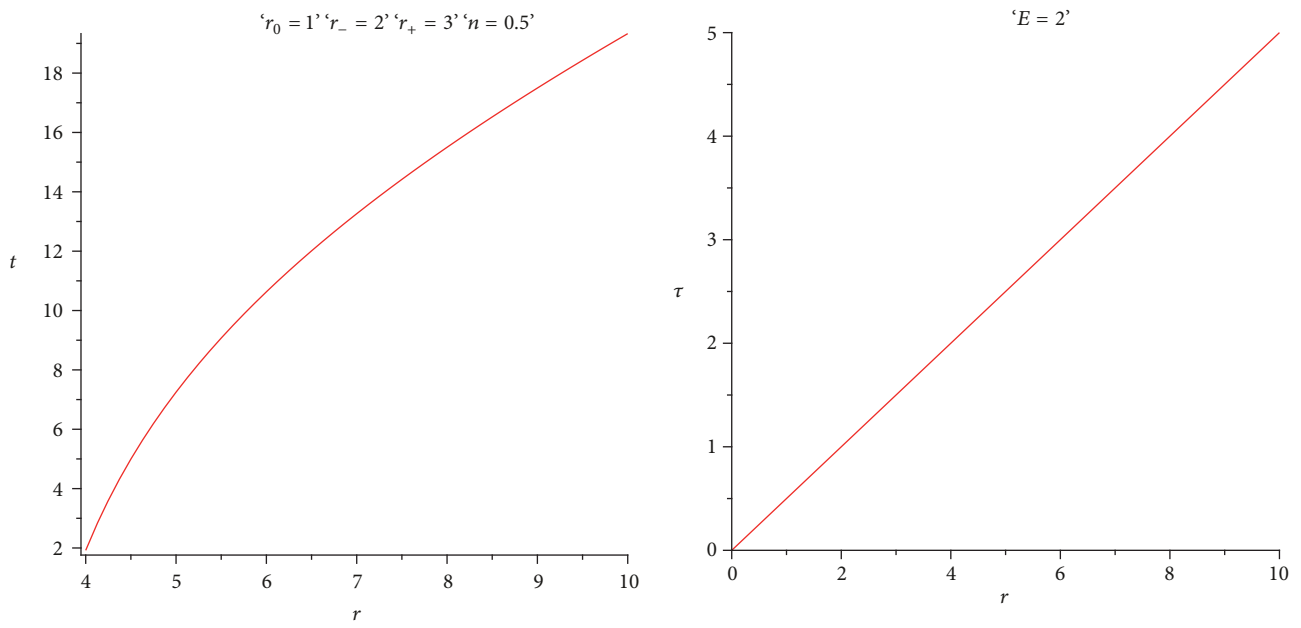

FIGURE 1: Graphs of $t - r$ (left) and $\tau - r$ (right) for a massless particle.

After integrating we get

$$\pm t = r + \frac{\ln(r - r_-)\, r^2}{r_- - r_+} - \frac{\ln(r - r_-)\, r_0^2}{r_- - r_+} - \frac{\ln(r - r_+)\, r_+^2}{r_- - r_+} + \frac{\ln(r - r_+)\, r_0^2}{r_- - r_+}. \tag{18}$$

Again from (14) we obtain for $L = 0$

$$\left(\frac{dr}{d\tau}\right)^2 = E^2, \tag{19}$$

from which we have a $\tau - r$ relationship

$$\pm\tau = \frac{r}{E}. \tag{20}$$

In Figure 1 (left) t is plotted with respect to the radial coordinate r and in Figure 1 (right) the proper time (τ) is plotted with respect to radial coordinate r for a massless particle.

3.2. Massive Particle Motion ($L = -1$). For a massive particle the Lagrangian L is -1 and from (14) and (15) we obtain for the motion of a massive particle the relationships between t and r and τ and r, respectively, as

$$\pm t = \int \frac{E\,dr}{\left((r - r_-)(r - r_+)/(r - r_0)^{(2-2n)}(r + r_0)^{2n}\right)\left(E^2 - (r - r_-)(r - r_+)/(r - r_0)^{(2-2n)}(r + r_0)^{2n}\right)^{1/2}} \tag{21}$$

$$\pm\tau = \int \frac{(r - r_0)^{(1-n)}(r + r_0)^n\, dr}{\left(E^2(r - r_0)^{(2-2n)}(r + r_0)^{2n} - (r - r_-)(r - r_+)\right)^{1/2}}. \tag{22}$$

In Figure 2 the graphs of t with respect to the radial coordinate r (left) and of the proper time τ with respect to the radial coordinate r (right) for a massive particle are presented.

4. The Effective Potential

From the geodesic equation (11) we have

$$\frac{1}{2}\left(\frac{dr}{d\tau}\right)^2 = \frac{1}{2}\left[E^2 - f(r)\left(\frac{J^2}{h(r)} - L\right)\right]. \tag{23}$$

After comparing the above equation with the well known equation $(1/2)(dr/d\tau)^2 + V_{\text{eff}} = 0$, we obtain the following expression for the effective potential:

$$V_{\text{eff}} = -\frac{1}{2}\left[E^2 - f(r)\left(\frac{J^2}{h(r)} - L\right)\right]. \tag{24}$$

From (24) one can see that the effective potential depends on the energy per unit mass, E, and the angular momentum, J.

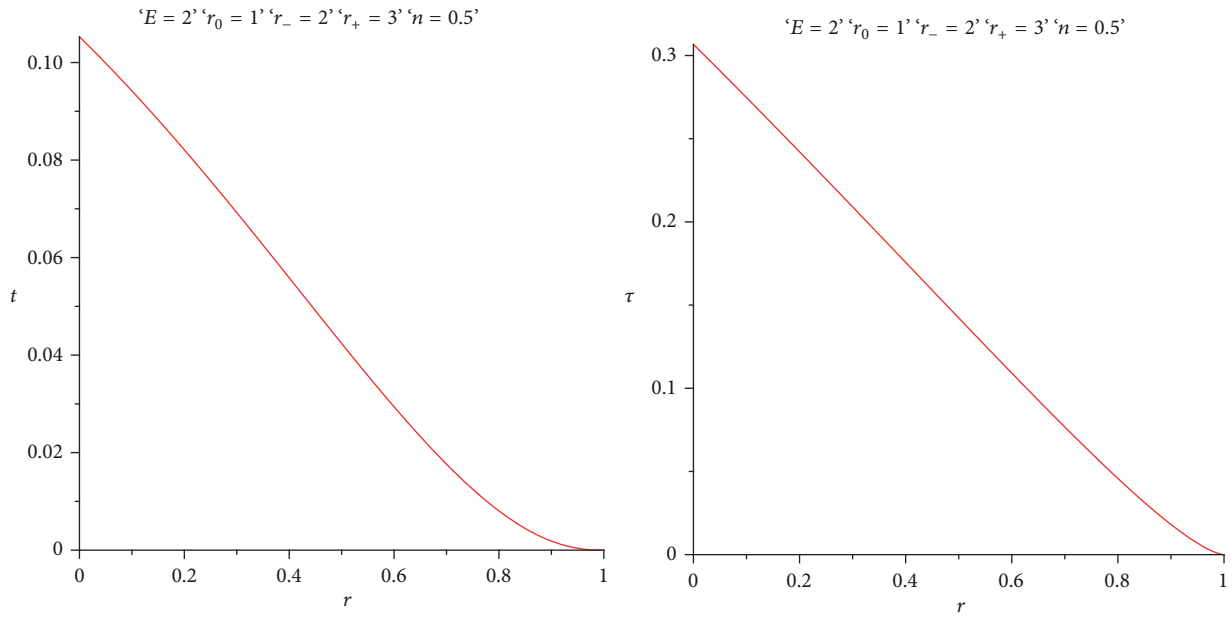

FIGURE 2: Graphs of $t - r$ (left) and $\tau - r$ (right) for a massive particle.

4.1. Massless Particle Case ($L = 0$). For the radial geodesics ($J = 0$), (24) yields

$$V_{\text{eff}} = -\frac{E^2}{2} \tag{25}$$

and the particle behaves like a free particle if $E = 0$.

Now we consider the circular geodesics ($J \neq 0$). The corresponding effective potential is given by

$$V_{\text{eff}} = -\frac{E^2}{2} + \frac{J^2}{2}\frac{(r - r_-)(r - r_+)}{(r + r_0)^{4n}}. \tag{26}$$

For $E \neq 0$ and $J = 0$ we infer from (26) that the effective potential does not depend on the charge and the mass of the black hole in generalized dilaton-axion gravity. The shape of the effective potential for $E \neq 0$ is shown in Figure 3 (left) for $J = 6$ (solid curve) and $J = 0$ (dotted line). We notice that for a nonzero value of J, the effective potential acquires a minimum, implying that stable circular orbits might exist. For $J = 0$, there are no stable circular orbits.

Now if we consider $E = 0$ and circular geodesics, i.e., $J \neq 0$, then, from (26), it is clear that the roots of the effective potential are the same as the horizon values. Further, the effective potential is negative between its two roots, i.e., between the horizons. Hence, since the effective potential has a minimum value stable circular orbits must exist, a conclusion that is confirmed in Figure 3 (right).

4.2. Massive Particle Case ($L = -1$). The effective potential for the massive particle is obtained from (24) as

$$V_{\text{eff}} = -\frac{1}{2}\left[E^2 - f(r)\left(\frac{J^2}{h(r)} + 1\right)\right]. \tag{27}$$

Now, for the radial geodesics with $J = 0$, $E = 0$, the above equation yields

$$V_{\text{eff}} = \frac{1}{2}\frac{(r - r_-)(r - r_+)}{(r - r_0)^{(2-2n)}(r + r_0)^{2n}}. \tag{28}$$

From (28) we notice that the solutions for the effective potential coincide with the horizon values for radial geodesics with $E = 0$, which is demonstrated graphically in Figure 4 (left). Further, from Figure 4 (left), one can see that the motion of the particle is bounded in the interior region of the black hole. The behaviour of the effective potential for $E \neq 0$ is depicted in the bottom part of Figure 4 (left). In this case, we also deduce that a bound orbit is possible for the massive particle.

Next we will consider the motion of a test particle with nonzero angular momentum. For $E = 0$, the roots of the effective potential coincide with the horizons (see Figure 4 (right)). Thus the particle is bounded in the interior region of the black hole.

5. Motion of a Test Particle

In this section we study the motion of a test particle of mass M and charge e in the gravitational field of a charged black hole in generalized dilaton-axion gravity. The Hamilton-Jacobi equation [11] is

$$g^{ik}\left(\frac{\partial S}{\partial x^i} + eA_i\right)\left(\frac{\partial S}{\partial x^k} + eA_k\right) + M^2 = 0, \tag{29}$$

where g_{ik}, A_i are the metric potential and the gauge potential, respectively, and S is Hamilton's standard characteristic

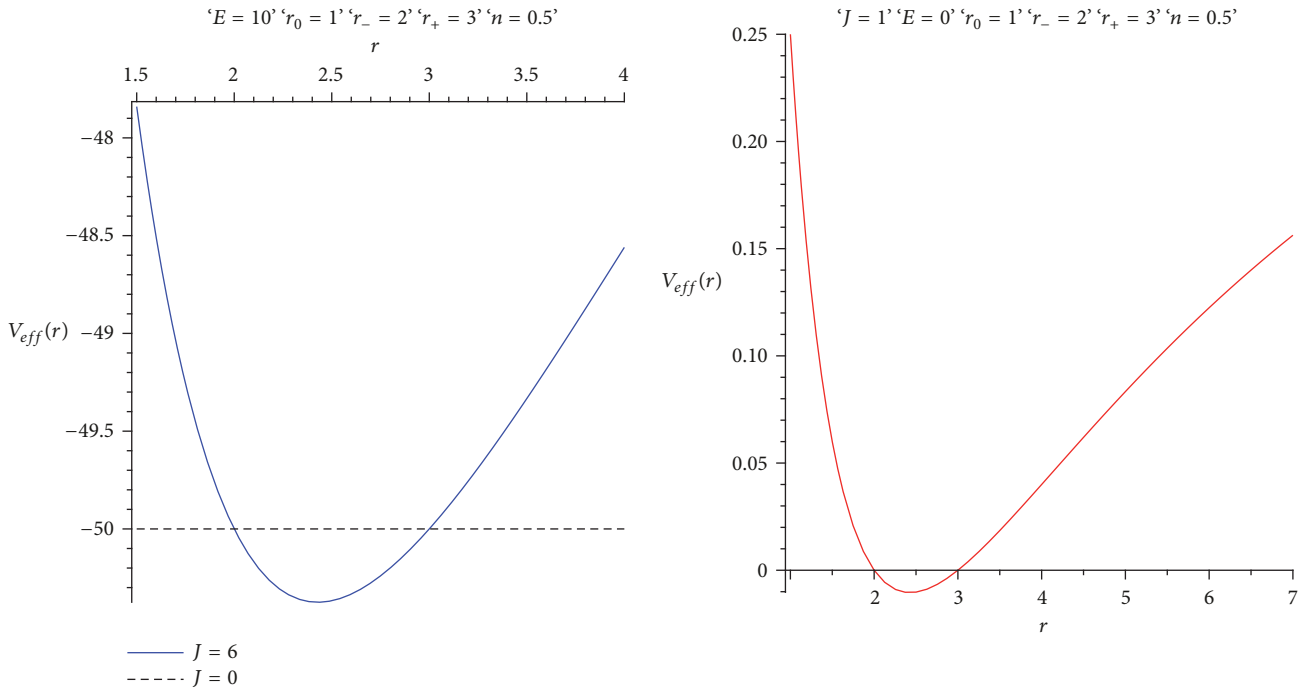

FIGURE 3: Graphs of $V_{\text{eff}} - r$ with $E = 10$, $J = 6$ and $J = 0$ (left) and $V_{\text{eff}} - r$ with $E = 0$ and $J = 1$ (right), for a massless particle.

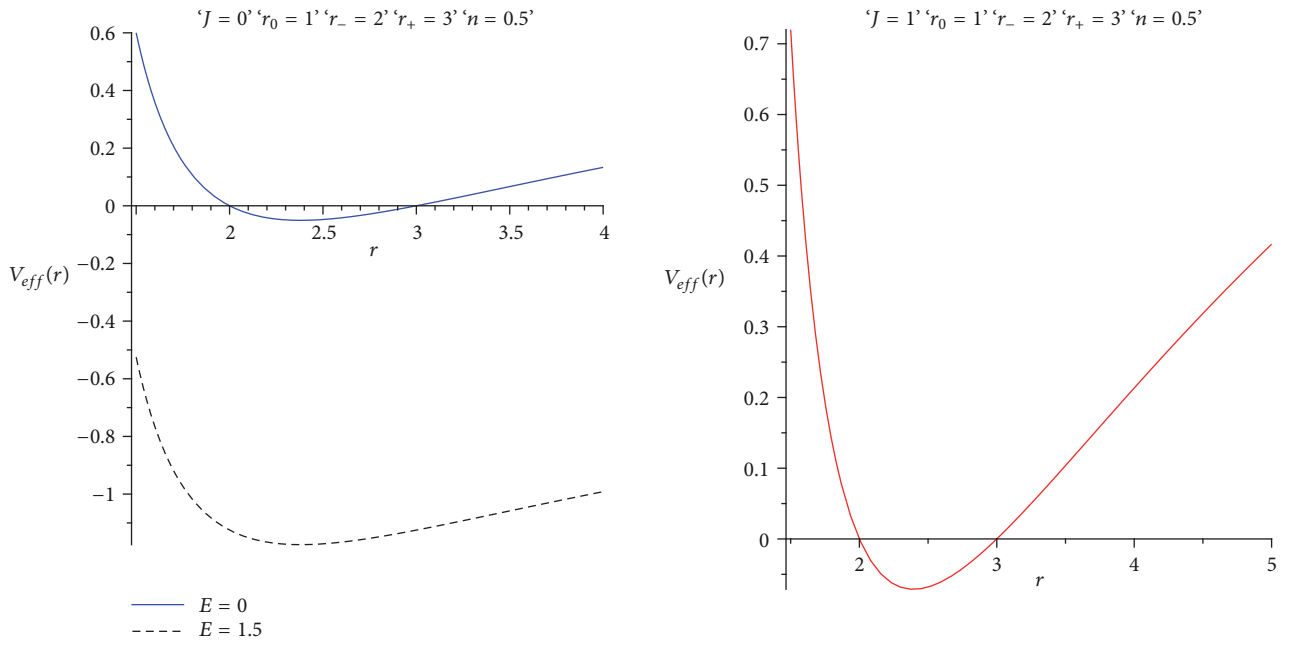

FIGURE 4: Graphs of $V_{\text{eff}} - r$ with $J = 0$, $E = 0$, and $E = 1.5$ (left) and $V_{\text{eff}} - r$ with $J = 1$ and $E = 0$ (right), for a massive particle.

function. The explicit form of the Hamilton-Jacobi equation for the line element (2) is

$$-\frac{1}{f(r)}\left(\frac{\partial s}{\partial t}+\frac{eQ}{r}\right)^2+f(r)\left(\frac{\partial S}{\partial r}\right)^2+\frac{1}{h(r)}\left(\frac{\partial S}{\partial \theta}\right)^2 + \frac{1}{h(r)\sin^2\theta}\left(\frac{\partial S}{\partial \phi}\right)^2+M^2=0, \tag{30}$$

where Q is the charge of the black hole. To solve the above partial differential equation, let us assume a separable solution in the form

$$S(t,r,\theta,\phi) = -Et + S_1(r) + S_2(\theta) + J\phi, \tag{31}$$

where E and J are the energy and angular momentum of the particle, respectively. After some simplification we obtain

$$S_1(r) = \epsilon \int \left[\frac{(E - eQ/r)^2}{f^2} - \frac{p^2}{fh} - \frac{M^2}{f} \right]^{1/2}, \quad (32)$$

$$S_2(\theta) = \epsilon \int \left(p^2 - J^2 \mathrm{cosec}^2\theta \right)^{1/2}, \quad (33)$$

where $\epsilon = \pm 1$ and p is the separation constant also known as the momentum of the particle.

The radial velocity of the particle is given by

$$\frac{dr}{dt} = f^2 \left(E - \frac{eQ}{r} \right)^{-1} \cdot \left[\frac{1}{f^2} \left(E - \frac{eQ}{r} \right)^2 - \frac{p^2}{fh} - \frac{M^2}{f} \right]^{1/2}. \quad (34)$$

The turning points of the trajectory are obtained by the vanishing of the radial velocity, $dr/dt = 0$, which yields

$$\left(E - \frac{eQ}{r} \right)^2 - \frac{p^2 f}{h} - M^2 f = 0. \quad (35)$$

After solving this equation for E, we get

$$E = \frac{eQ}{r} + \sqrt{f} \left(\frac{p^2}{h} + M^2 \right)^{1/2}. \quad (36)$$

The effective potential is obtained from the relation $V(r) = E/M$ as follows:

$$V = \frac{eQ}{Mr} + \sqrt{f} \left(\frac{p^2}{M^2 h} + 1 \right)^{1/2}. \quad (37)$$

Using (3) and (4) the effective potential becomes

$$V(r) = \frac{eQ}{Mr} + \left(1 + \frac{p^2 (r - r_0)^{2n-2}}{M^2 (r + r_0)^{2n}} \right) \cdot \left(\frac{\sqrt{(r - r)(r - r_+)}}{(r - r_0)^{1-n} (r + r_0)^n} \right). \quad (38)$$

In the stationary system ($dV/dr = 0$) we obtain

$$\begin{aligned} &- \frac{eQ}{Mr^2} + \frac{1}{2} \frac{\left((r - r_-)(r - r_+)\right)^{1/2} \left(p^2 (r - r_0)^{2n-2} (2n - 2)/M^2 (r - r_0)(r + r_0)^{2n} - 2p^2 n (r - r_0)^{2n-2}/M^2 (r + r_0)^{2n+1} \right)}{\left(1 + p^2 (r - r_0)^{2n-2}/M^2 (r + r_0)^{2n} \right)^{1/2} (r - r_0)^{1-n} (r + r_0)^n} \\ &+ \frac{1}{2} \frac{(2r - r_+ - r_-) \left(1 + p^2 (r - r_0)^{2n-2}/M^2 (r + r_0)^{2n} \right)^{1/2}}{\left((r - r_-)(r - r_+)\right)^{1/2} (r - r_0)^{1-n} (r + r_0)^n} \\ &- \frac{(1 - n) \left(1 + p^2 (r - r_0)^{2n-2}/M^2 (r + r_0)^{2n} \right)^{1/2} \left((r - r_-)(r - r_+)\right)^{1/2}}{(r - r_0)^{2-n} (r + r_0)^n} \\ &- \frac{n \left(1 + p^2 (r - r_0)^{2n-2}/M^2 (r + r_0)^{2n} \right)^{1/2} \left((r - r_-)(r - r_+)\right)^{1/2}}{(r - r_0)^{1-n} (r + r_0)^{n+1}} = 0. \end{aligned} \quad (39)$$

In order to use a more simplified equation and thus be able to visualize it by plotting its graph, one may select some specific value for n. Here we choose $n = 0.5$ (since $0 < n < 1$) and the simplified form of equation (39) is given by

$$\begin{aligned} &\alpha(r) \\ &:= \frac{2eQ \left(r^2 - r_0^2 \right)^{1/2}}{Mr^2} \\ &+ \frac{2r \left((r - r_-)(r - r_+)\right)^{1/2}}{(r^2 - r_0^2)} \left(\frac{p^2}{M^2 (r^2 - r_0^2) \beta} + \beta \right) \\ &- \frac{(2r - r_+ - r_-) \beta}{\left((r - r_-)(r - r_+)\right)^{1/2}} = 0, \end{aligned} \quad (40)$$

where $\beta = (1 + p^2/M^2(r^2 - r_0^2))^{1/2}$.

5.1. Test Particle in Static Equilibrium. The momentum p must be zero in the static equilibrium system; thus from (40) we get

$$\begin{aligned} &\left(4e^2Q^2 - M^2 \left(2r_-r_+ + r_+^2 - r_-^2 \right) \right) r^8 \\ &+ \left(-4e^2Q^2 (r_- + r_+) \right. \\ &\left. + 4M^2 \left(r_0^2 r_- + r_0^2 r_+ r_-^2 r_+ + r_- r_+^2 \right) \right) r^7 \\ &+ \left(4e^2Q^2 \left(r_-r_+ - 3r_0^2 \right) \right. \\ &\left. - 2M^2 \left(6r_0^2 r_-r_+ + r_0^2 r_-^2 + r_-^2 r_+^2 + r_0^2 r_+^2 - r_0^4 \right) \right) r^6 \\ &+ \left(12e^2Q^2 r_0^2 (r_- + r_+) \right. \\ &\left. + 4M^2 r_0^2 \left(r_+ r_-^2 + r_+^2 r_- + r_0^2 (r_+ + r_-) \right) \right) r^5 \end{aligned}$$

$$+\left(12e^2Q^2r_0^2\left(r_0^2-r_+r_-\right)\right.$$
$$\left.-M^2r_0^4\left(2r_+r_-+r_+^2+r_-^2\right)\right)r^4-12e^2Q^2r_0^4\left(r_++r_-\right)$$
$$\cdot r^3+4e^2Q^2r_0^4\left(3r_+r_--r_0^2\right)r^2+4e^2Q^2r_0^6\left(r_++r_-\right)$$
$$\cdot r-4e^2Q^2r_0^6r_+r_-=0. \tag{41}$$

We notice that the last term of the above equation is negative. So, this equation has at least one positive real root. Consequently, a bound orbit is possible for the test particle, i.e., the test particle can be trapped by a charged black hole in generalized dilaton-axion gravity. In other words, a charged black hole in generalized dilaton-axion gravity exerts an attractive gravitational force on matter.

5.2. Test Particle in Nonstatic Equilibrium

5.2.1. Test Particle without Charge ($e = 0$). In this case (40) becomes

$$M^2\left(r_-+r_+\right)r^4-2\left(r_0^2M^2+r_-r_+M^2+p^2\right)r^3$$
$$+3p^2\left(r_+-r_-\right)r^2$$
$$+2\left(r^4M^2-r_0^2p^2+r_0^2M^2r_+r_--2p^2r_+r_-\right)r \tag{42}$$
$$+r_0^2\left(r_+p^2+r_-p^2-M^2r_0^2r_+-M^2r_0^2r_-\right)=0.$$

If $M^2r_0^2r_+ + M^2r_0^2r_- > r_+p^2 + r_-p^2$, one can see that the last term of the above equation is negative. Therefore, this equation must have at least one positive real root. Consequently, a bound orbit for the uncharged test particle is possible. If $M^2r_0^2r_+ + M^2r_0^2r_- = r_+p^2 + r_-p^2$, then (42) changes to a third-degree equation with two changes of sign. By Descarte's rule of sign, this equation must have either two positive roots or no positive roots at all. Thus, a bound orbit for the uncharged test particle may or may not be possible. For $M^2r_0^2r_+ + M^2r_0^2r_- < r_+p^2 + r_-p^2$, (42) has two changes of sign. Here, again a bound orbit for the uncharged test particle may or may not be possible.

5.2.2. Test Particle with Charge ($e \neq 0$). For a charged test particle with $n = 0.5$, the stationary system ($dV/dr = 0$) yields the form given in (40). As this equation is algebraically very complicated, we use the graph of $\alpha(r)$ in order to find out whether there exist any real positive roots. From Figure 5 one can see that, for different values of the test particle's charge, $\alpha(r)$ given by (40) does not intersect the r-axis. Hence, no real positive roots are possible. As a result, no bound orbit for the charged test particle is possible.

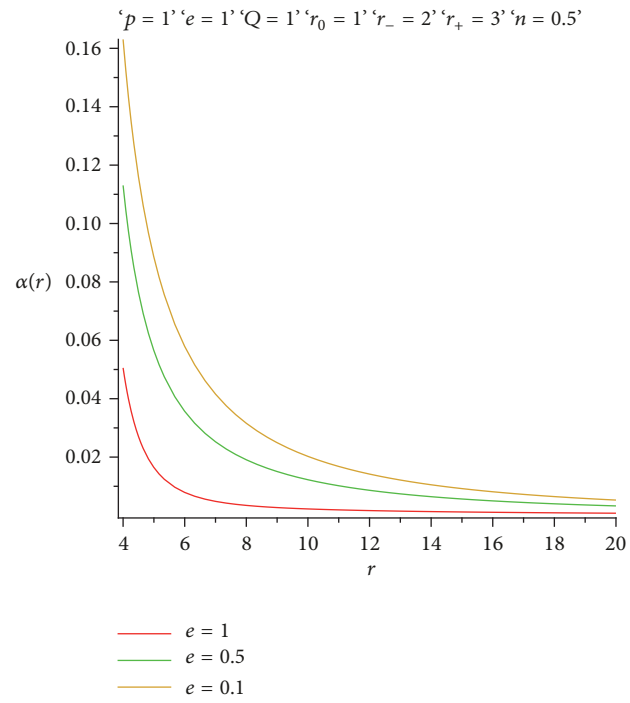

FIGURE 5: Graph of $\alpha(r)$ given in (40) for different values of the test particle's charge.

6. Discussion

In the present investigation, we have analyzed the behaviour of massless and massive particles in the gravitational field of a charged black hole in generalized dilaton-axion gravity in four dimensions. To this purpose, we have studied the motion of a massless particle ($L = 0$) and a massive particle ($L = -1$). We have plotted the graphs of t and the proper time τ with respect to the radial coordinate r. For the massless particle t increases nonlinearly with r (Figure 1 (left)), while the proper time τ increases linearly with r (Figure 1 (right)). In the case of the massive particle motion both t and τ decrease nonlinearly with r (Figure 2).

Further, studying the effective potential we ended up with (24) from which we conclude that V_{eff} depends on the energy per unit mass E and the angular momentum J. For a massless test particle we found that $V_{\text{eff}} = -E^2/2$ in the case of radial geodesics ($J = 0$), while if $E = 0$ the particle behaves like a free particle. In the case of circular geodesics ($J \neq 0$), V_{eff} is given by (26). In Figure 3 the behaviour of V_{eff} is presented for zero and nonzero E and various values of J. From these graphs it can be inferred that for $E \neq 0$ and $J \neq 0$ the effective potential V_{eff} has a minimum and circular orbits are possible, while for $E \neq 0$ and $J = 0$ no stable circular orbits can exist. In the cases $E = 0$ and $J \neq 0$ the effective potential V_{eff} changes sign two times between the horizons and stable circular orbits must exist.

From the examination of the calculated effective potential, (27) for a massive particle, we have considered the radial geodesics for the cases $J = 0$ and $E = 0$, $J = 0$ and $E \neq 0$, and $J \neq 0$ and $E = 0$. It is seen (Figure 4) that in the first case the roots of the effective potential coincide with the horizons' positions and the particle's orbit is bound in the black hole's interior. In the second case, a bound orbit is also possible. Finally, in the third case, i.e., when the particle's angular momentum does not vanish, the roots of the effective

potential coincide again with the horizons' positions and the particle's orbit is bound again in the black hole's interior.

As a last step we have examined the motion of a massive and charged test particle in the gravitational field of a charged black hole in generalized dilaton-axion gravity by exploiting the Hamilton-Jacobi equation. The latter is set up for the space-time geometry considered and is analytically solved by applying additive separation of variables. As a result, the particle's radial velocity and the effective potential are determined in closed form. Then the case of static equilibrium is examined and it is found that the charged test particle may have a bound orbit; i.e., it can be trapped by a charged black hole in this context or, stated differently, the charged black hole exerts an attractive gravitational force upon the charged particle in generalized dilaton-axion gravity. In the case of nonstatic equilibrium, we have distinguished between an uncharged and a charged test particle. In the former case, conditions have been found for the possibility of existence of the particle's bound orbit. Finally, when the test particle carries a charge, it is seen graphically (Figure 5) that no bound orbit is possible.

An interesting perspective for future work would be the study of the motion of charged or uncharged test particles and the behaviour of geodesics for rotating black hole solutions or for black hole solutions in more than four space-time dimensions in the context of generalized dilaton-axion gravity.

Data Availability

The data used to support the findings of this study are available from the corresponding author upon request.

Conflicts of Interest

The authors declare that they have no conflicts of interest.

Acknowledgments

Farook Rahaman would like to thank the authorities of the Inter-University Centre for Astronomy and Astrophysics, Pune, India, for providing research facilities. Farook Rahaman and Susmita Sarkar are also grateful to DST-SERB (Grant No.: EMR/2016/000193) and UGC (Grant No.: 1162/(sc)(CSIR-UGC NET, DEC 2016)), Govt. of India, for financial support, respectively.

References

[1] T. Ortín, *Gravity and Strings*, Chapter 16, Cambridge University Press, 2004.

[2] S. Sur, S. Das, and S. SenGupta, "Charged black holes in generalized dilaton-axion gravity," *Journal of High Energy Physics*, vol. 10, article no. 064, 2005.

[3] T. Ghosh and S. SenGupta, "Thermodynamics of dilation-axion black holes," *Physical Review D*, vol. 78, no. 12, Article ID 124005, 2008.

[4] A. A. Usmani, Z. Hasan, F. Rahaman, S. A. Rakib, S. Ray, and P. K. Kuhfittig, "Thin-shell wormholes from charged black holes in generalized dilaton-axion gravity," *General Relativity and Gravitation*, vol. 42, no. 12, pp. 2901–2912, 2010.

[5] I. Radinschi, F. Rahaman, and A. Ghosh, "On the energy of charged black holes in generalized dilaton-axion gravity," *International Journal of Theoretical Physics*, vol. 49, no. 5, pp. 943–956, 2010.

[6] Z. M. Yang, X.-L. Li, and Y. Gao, "Entanglement entropy of charged dilaton-axion black hole and quantum isolated horizon," *European Physical Journal Plus*, vol. 131, no. 9, p. 304, 2016.

[7] T. Ghosh and S. SenGupta, "Tunneling across dilaton-axion black holes," *European Physics Letters*, vol. 120, no. 5, Article ID 50003, 2017.

[8] A. S. Bhatia and S. Sur, "Dynamical system analysis of dark energy models in scalar coupled metric-torsion theories," *International Journal of Modern Physics D*, vol. 26, no. 13, Article ID 1750149, 2017.

[9] S. Sur and A. S. Bhatia, "Weakly dynamic dark energy via metric-scalar couplings with torsion," *Journal of Cosmology and Astroparticle Physics*, vol. 2017, no. 7, p. 39, 2017.

[10] M. Kalam, F. Rahaman, and S. Mondal, "Particle motion around tachyon monopole," *General Relativity and Gravitation*, vol. 40, no. 9, pp. 1849–1861, 2008.

[11] S. Chakraborty and M. F. Rahaman, "Motion of test particles around gauge monopoles or near cosmic strings considering semiclassical gravitational effects," *International Journal of Modern Physics D*, vol. 9, no. 2, pp. 155–159, 2000.